

## LABORATORY OXIDATION OF FOSSIL ORGANIC MATTER STUDIED BY *in situ* INFRARED SPECTROSCOPY, ROCK-EVAL PYROLYSIS AND PYROLYSIS-GAS CHROMATOGRAPHY-MASS SPECTROMETRY

Jiri CEJKA<sup>a1</sup>, Zdenek SOBALIK<sup>a2</sup> and Bohdan KRIBEK<sup>b</sup>

<sup>a</sup> J. Heyrovsky Institute of Physical Chemistry, Academy of Sciences of the Czech Republic, 182 23 Prague 8, Czech Republic; e-mail: <sup>1</sup>cejka@jh-inst.cas.cz, <sup>2</sup>sobalik@jh-inst.cas.cz

<sup>b</sup> Czech Geological Survey, Klárov 3, 118 21 Prague 1, Czech Republic

Received October 3, 1996

Accepted January 19, 1997

*Dedicated to Dr Karel Mach on the occasion of his 60th birthday.*

Fossil organic matter in Miocene and Silurian sediments was subjected to experimental oxidation, which was investigated by Rock-Eval pyrolysis, the "off-line" pyrolysis-gas chromatography-mass spectrometry combination, and continuous FTIR monitoring. The pyrolysate yield decreased during the oxidation particularly in the low-matured, predominantly aliphatic organic matter from the Miocene sediments (type I kerogen, algae-type kerogen). This suggests that aliphatic chains are preferentially oxidized, which is in agreement with the marked decrease in the intensity of the  $\nu(\text{CH}_2)$  and  $\nu(\text{CH}_3)$  IR bands. The n-alkane distribution in the chromatographic profile was unaffected by the oxidation; hence, the oxidation of the alkane chains was not selective. At the same time, the bands within the 1 900–1 550  $\text{cm}^{-1}$  range grew in intensity for both the aliphatic and mixed-type (type II kerogen) organic matter. The oxidation of the aromatic (humic) type of organic fossil matter in the Miocene sediments (type III kerogen, coal-type kerogen) was only accompanied by very small changes in the FTIR spectra. The results of the "off-line" pyrolysis are consistent with those of the Rock-Eval pyrolysis. For all samples, the oxidation was accompanied by a gradual decrease in the hydrogen index (HI) as well as in the pyrolysis temperature maximum ( $T_{\text{max}}$ ). The changes in the  $S_2/S_1$  ratio ("bound"-to-"free" hydrocarbons) indicate that the "free" hydrocarbons in the rocks are preferentially oxidized during the first 8–16 h of the experimental run. Subsequently, hydrocarbon chains involved in the kerogen macromolecule are attacked.

**Key words:** *in situ* FTIR monitoring; Fossil organic matter; Pyrolysis-GC-MS.

Low-temperature oxidation of coal has been studied extensively because this process brings about substantial changes in the chemical, optical and technological properties of the substance. This is associated, *e.g.*, with a decrease in the yield of pyrolysis and, from practical point of view, with a decrease in the calorific value and lower yields during coal liquefaction<sup>1-3</sup>.

The effect of natural weathering is not well understood yet, and low-temperature laboratory oxidation is one of the possible ways to model this natural process under

controlled conditions. Various experimental techniques have been applied to the monitoring of laboratory low-temperature oxidation of different types of bitumenous and humic coals (FTIR (refs<sup>4,5</sup>), EPR (ref.<sup>6</sup>), DTA (refs<sup>7,8</sup>), ESCA (ref.<sup>8</sup>), <sup>13</sup>C NMR (ref.<sup>9</sup>)). This contribution is focused on the investigation of the experimental oxidation of fossil organic matter of different origin and thermal maturation, dispersed in sedimentary rocks<sup>10</sup>. This dispersed organic matter, usually referred to as "kerogen", consists of organic solvent-soluble and insoluble parts. The soluble part involves "free" hydrocarbons, whereas the insoluble part is mainly composed of "polycondensed" or "polymerized" organic matter (geopolymers) which includes "bound" hydrocarbons of both aliphatic and aromatic type. With respect to its source, kerogen is usually classified as type I (predominantly aliphatic, poor in oxygen, algae-derived), type II (mixed type) and type III (predominantly aromatic, rich in oxygen and poor in hydrogen, terrestrial plants-derived, coal type)<sup>11</sup>. Prior to oxidation tests, such dispersed organic matter is usually separated from rocks by acid leaching and preconcentrated. This process, however, alters the chemical composition of the organic matter to an unknown extent. Therefore, in our experiments the organic matter under investigation was oxidized without any chemical pretreatment.

In this study, the compositional and structural changes caused by low-temperature laboratory oxidation of fossil organic matter (kerogen) of different origin and degree of thermal maturation were investigated by Rock-Eval pyrolysis and by the "off-line" pyrolysis-gas chromatography-mass spectrometry combination using samples heated at 150 °C for 14 days. The results are compared with those of *in situ* FTIR experiments performed in a flow cell at 190 °C in an oxygen-enriched atmosphere.

## EXPERIMENTAL

### Materials

Three samples of organic matter rocks were used for experimental oxidation: Sample **A** – claystone from a Cypris Formation of Miocene Age (Sokolov Coal Basin), sample **B** – coal claystone from the footwall of the Antonin Seam, Main Seam Formation, Miocene (Sokolov Coal Basin), and sample **C** – black shale from the Koneprusy Formation, Silurian (Beroun Basin). The principal characteristics of the fresh organic matter used in the experiments, *viz.* total organic carbon (TOC), hydrogen and nitrogen concentration relative to carbon, hydrogen index (*HI*), and temperature maxima in the Rock-Eval pyrolysis, are given in Table I. The random reflectivity of organic matter (which increases with increasing thermal maturation of the organic matter during burial) is also included in this Table. Sample **A** represents low-matured, predominantly aliphatic kerogen (type I), sample **B** is of mixed type (kerogen II type). Sample **C** cannot be classified unambiguously due to its high degree of thermal maturation.

### Apparatus

Huminite/vitrinite reflectance in incident light was studied on an UMSP 30 microscope-microphotometer (Opton, Zeiss) with the immersion objective on the leaf section. The measurements were

carried out at the Institute of Rock Mechanics and Structure, Academy of Sciences of the Czech Republic in Prague.

Laboratory oxidation of the fossil organic matter was conducted in static conditions in air at 150 °C for 8–256 h.

Rock–Eval pyrolysis was performed in laboratories of the Czech Geological Survey, Brno Branch, using a Rock–Eval 5 pyrolyser. The sample (0.05–0.1 g) in an inert atmosphere was first heated to 300 °C, and the concentration of evolved organic compounds (“free” hydrocarbons  $S_1$ ) was measured for 15 min by using a flame ionization detector. Subsequently, the sample was heated to 550 °C at 25 °C/min. All volatilized compounds evolved during this pyrolysis process are assumed to arise from the degradation of the insoluble part of kerogen, “bound” hydrocarbons  $S_2$ . The values of  $S_1$  and  $S_2$  were also used to estimate the hydrogen index in total organic carbon. The maximum pyrolysis temperature was used for characterization of the maturation state of the fossil organic matter.

“Off-line” pyrolysis was carried out in a fixed bed glass reactor. The samples (2 g) were heated at a pressure of 660 Pa using a temperature programme of 8 °C/min up to a temperature above 450 °C. The volatile products were condensed in a glass receiver which was cooled at 0 °C. Details of the pyrolysis experiments have been described and the effect of the pyrolysis conditions on the chromatographic profiles has been discussed elsewhere<sup>12,13</sup>.

The liquid pyrolysis products were analyzed on a Hewlett–Packard 5890 Series II gas chromatograph and identified using a Hewlett–Packard 5971A quadruple mass spectrometric detector. The separation was performed by using a high resolution capillary column (SPB-1, Supelco, 30 m, i.d. 0.2 mm, film thickness 0.2 µm). Injector and detector temperatures were set at 250 °C. The temperature programme run from 60 to 275 °C at a rate of 5 °C/min. The mass spectrometer was calibrated with perfluorotributylamine (PFTBA), and the spectra were recorded in the electron impact mode at an ionisation energy of 70 eV over the  $m/z$  range of 25–450. Standards of individual substances ( $C_{25}H_{52}$ ,  $C_{28}H_{58}$ ,  $C_{30}H_{62}$ ,  $C_{33}H_{68}$ , Fluka) and a spectral library were used to elucidate the spectra recorded.

The oxidation experiments in a flow cell were monitored using a Magna 550 FTIR spectrometer (Nicolet, U.S.A.). The description of the cell will be published elsewhere<sup>14</sup>. The samples were prepared by pressing about 30 mg of the finely ground material into thin self-supported wafers 30 × 10 mm in size. For samples **A** and **B**, their mechanical properties enabled the pressed wafer of the optimum thickness to be obtained. All spectra were normalized to a sample weight equivalent to 10 mg/cm<sup>2</sup> of the pressed sample. The following procedure was used for the oxidation of organic matter in the FTIR flow cell. The samples were dried *in situ* in the cell in pure nitrogen (15 ml/min) while the temperature was increased to 190 °C at a rate of 3–5 °C/min and then held at this temperature for an hour. After that time, the oxidation was started by adding 15 ml/min of oxygen to the nitrogen stream to reach the nitrogen/oxygen = 1 : 1 ratio. The oxidation was monitored for about 10 h. IR spectra were recorded every 15–30 min with 300 scans at a resolution of 2 cm<sup>-1</sup>. In each record, the

TABLE I  
Geochemical and optical characteristic of samples subjected to oxidation experiments

Sample	TOC, wt.%	H/C <sub>at</sub>	N/C <sub>at</sub>	HI, mg HC/g TOC	T <sub>max</sub> , °C	R <sub>r</sub> , %
<b>A</b>	4.4	1.60	0.02	653	434	0.39
<b>B</b>	16.0	1.01	0.01	286	416	0.41
<b>C</b>	2.34	0.75	0.03	156	448	0.98

spectrum of the dry sample before oxidation was subtracted. The standard routine procedure consisting of identification of the band positions using Fourier self-deconvolution and/or the second derivative mode was applied to analyze overlapping bands. The band separation was based on the assumption of their Gauss profile, and the least-square minimalization procedure was employed.

## RESULTS AND DISCUSSION

### Rock–Eval Pyrolysis and Hydrogen Index

The decrease in the liquid pyrolysate yield can be correlated with the decrease in the hydrogen index (*HI*) derived from the Rock–Eval pyrolysis. The results of the pyrolysis expressed in terms of *HI* and  $T_{\max}$  are given in Fig. 1. The *HI* values are seen to decrease substantially as the experimental oxidation proceeds. Moreover sample **C** exhibited a substantial shift of the  $T_{\max}$  value during the oxidation, whereas for samples **A** and **B** the shift was not very pronounced. The  $S_2/S_1$  ratio (“bound”/“free” hydrocarbons) increased during the first 16 h of laboratory oxidation, particularly for sample **A** (Fig. 2). This indicates that mainly “free” hydrocarbons in the rocks were preferentially

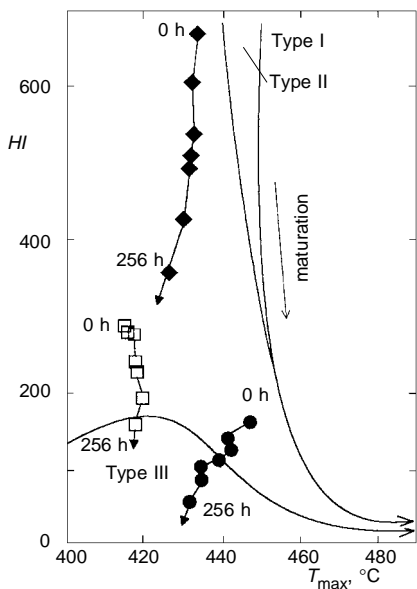


FIG. 1

Oxidation of organic matter in samples A–C expressed in terms of the Rock–Eval hydrogen index (*HI*) and temperature maximum of the pyrolysate yield. The maturation paths are also given for kerogen type I (aliphatic), II (mixed), and III (aromatic). Sample:  $\blacklozenge$  A,  $\square$  B,  $\bullet$  C

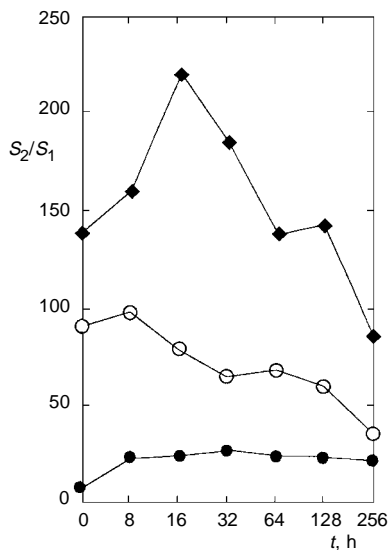


FIG. 2

Time dependence of the  $S_2/S_1$  ratio during the laboratory oxidation. Sample:  $\blacklozenge$  A,  $\square$  B,  $\bullet$  C

vaporized and/or oxidized during this period in contrast to hydrocarbons bound in the kerogen macromolecule. Apparently the more aliphatic hydrocarbons are present in the organic matter the higher is the increase in the  $S_2/S_1$  ratio during the first hours of oxidation (Fig. 2). After this initial oxidation period, hydrocarbons forming a part of the kerogen macromolecule are oxidized, which is related to the gradual decrease in the  $S_2/S_1$  ratio for the remaining part of the run. From the Rock-Eval pyrolysis data it can be inferred that although the fresh fossil organic matter differs in the aliphatic-to-aromatic hydrocarbon ratio, the organic matter remaining after a long time of oxidation can be very similar. For sample **C** both the pyrolysis yield and the  $S_2/S_1$  ratio underwent very small changes during oxidation. This suggests that the bulk of this highly thermal matured organic matter is resistant to further oxidation because both the "free" aliphatic hydrocarbon chains and hydrocarbons "bound" to the kerogen macromolecule were already split off in the course of the natural thermal maturation.

#### "Off-Line" Pyrolysis-Gas Chromatography-Mass Spectrometry

The results of the oxidation experiments are summarized in Table I and Figs 1–3. The amount of liquid pyrolysate decreases gradually during the experimental run (Fig. 3). The highest value of liquid pyrolysate of 500 mg/g TOC was found for sample **A**, which contains immature organic matter predominantly of the aliphatic (algae) type. The liquid pyrolysate yields during the first 8–64 h were lower for sample **B** (aliphatic-aromatic mixed type) and lowest for sample **C** containing highly matured organic matter. In 128 h the pyrolysate yields for samples **A** and **B** were similar, although the rates

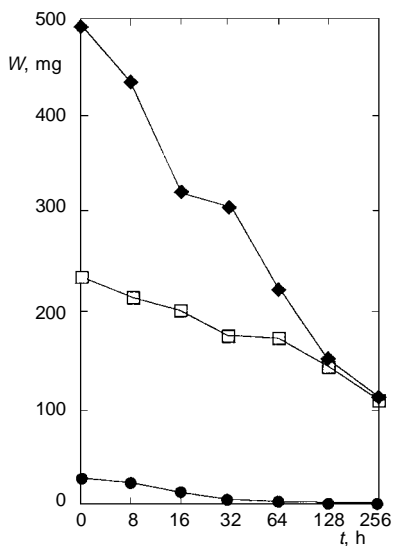


FIG. 3  
Time dependence of the liquid pyrolysate yield  $w$  (in mg pyrolysate per g TOC) during oxidation. Sample:  $\blacklozenge$  **A**,  $\square$  **B**,  $\bullet$  **C**

of pyrolysis were highly different. Both samples are of the same degree of maturation and differ only in their chemical composition. This indicates that mostly aliphatic chains that are oxidized during the laboratory oxidation. Due to the high degree of

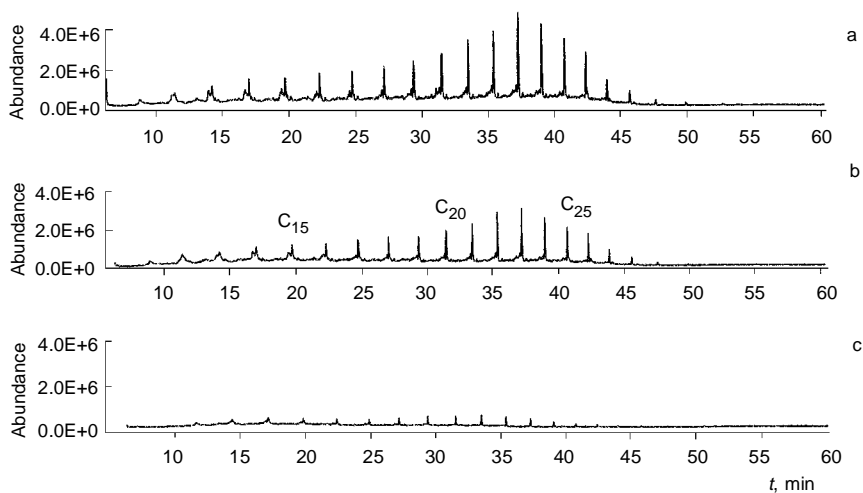


FIG. 4  
Chromatographic profiles of the liquid pyrolysis products of sample **A**. Time of oxidation (h): a 0, b 32, c 256

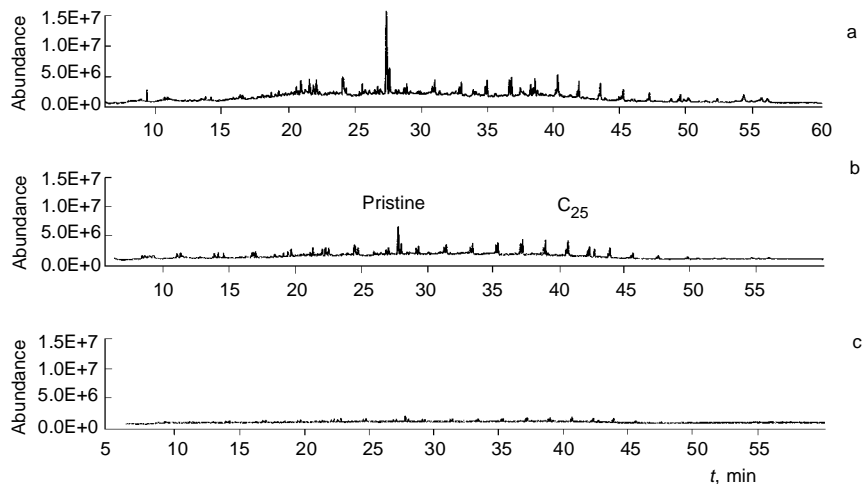


FIG. 5  
Chromatographic profiles of the liquid pyrolysis products of sample **B**. Time of oxidation (h): a 0, b 32, c 256

thermal maturation of sample **C**, the decrease in the pyrolysate yield was less marked than for the immature organic matter of the Tertiary age.

All three samples of fossil organic matter were investigated with respect to the distribution of organics in their pyrolysis products, using gas chromatography with mass spectrometric detection. Typical changes in the chromatographic profiles for samples **A** and **B** are shown in Figs 4 and 5. The concentration of organics in the pyrolysis product of sample **C** was below the detection limit of the mass spectrometer. In accordance with the results of Rock–Eval pyrolysis, a substantial decrease in the pyrolysis yields was observed during the oxidation. On the other hand, no particular changes in the distribution of long-chain alkanes were observed for the oxidized samples. This is in a good agreement with the results obtained by Anderson and Johns<sup>15</sup>, who observed non-preferential loss of aliphatic material during low-temperature oxidation of Australian coals. The authors reported that significant amounts of C<sub>1</sub>–C<sub>9</sub> aliphatic hydrocarbons evolved in the initial steps of the oxidation. A fraction of these compounds seems to be adsorbed in the material, which was also observed in the FTIR cell during the heating of the sample in an inert atmosphere. However, their release was observed for the extended period of time, which can be explained so that they are also evolved from the coal macromolecules during oxidation. This indicates that there is no preferential oxidation of a particular fraction of the fossil organic matter, and it can be inferred that the “free” hydrocarbons are preferentially oxidized and/or volatilized during the first hours of the laboratory oxidation, which is in line with the S<sub>2</sub>/S<sub>1</sub> hydrocarbon ratio. Thus, this process seems to be much faster than the subsequent oxidation of “bound” hydrocarbons.

### *In situ Oxidation Studied by FTIR*

Prior to oxidation, the pressed samples were heated to about 190 °C in a flow of dry nitrogen in order to remove physically adsorbed water. Apparently, some amount of the short-chain hydrocarbons was lost during process (estimated to about 20% for sample **B**). The changes in the aliphatic content during oxidation are reflected in the IR region of 3 050 to 2 750 cm<sup>-1</sup> (Figs 6a, 6b), displaying a complex band which can be resolved into five individual components (Fig. 6c) and assigned according to Painter *et al.*<sup>5</sup> to stretching vibrations of CH<sub>3</sub>, CH<sub>2</sub> and CH groups (Table II). The intensity of a band at 2 855 cm<sup>-1</sup> was used to evaluate the consumption of the aliphatic species during the oxidation. Composed of two individual bands (see Table II and Fig. 6c), this complex band reflects conveniently changes in both the CH<sub>3</sub> and CH<sub>2</sub> contents. Simultaneously with the decrease in the intensity of bands of stretching vibrations of the CH<sub>2</sub> and CH<sub>3</sub> groups, new bands appeared in the region of 1 850–1 550 cm<sup>-1</sup> due to the formation of various oxidation products.

The time dependence of the consumption of the alkyl species (long-chain alkanes) during the oxidation is shown in Fig. 7. The curves for samples **A** and **B** exhibit a rather steep decrease at the first stage of oxidation (up to about 50 min) followed by a longer

period of smaller changes even after prolongation of the oxidation period. The pyrolysis yields display a similar trend. Despite the much higher TOC value for the mixed sample **B** than for sample **A**, but in accordance with the character of the organic matter in sample **B**, the absolute amount of aliphatic species was estimated to be about 2.5 times lower in sample **B** than in sample **A**.

Using the  $2956\text{ cm}^{-1}/2924\text{ cm}^{-1}$  band intensity ratio for evaluation of the  $\text{CH}_3/\text{CH}_2$  ratio, the relative length of the aliphatic chains was found to decrease during the oxidation for both samples (the  $2956\text{ cm}^{-1}/2924\text{ cm}^{-1}$  lowered from 0.45 to 0.41 for samples **A** and from 0.80 to 0.71 for sample **B**). The substantially higher  $\text{CH}_3/\text{CH}_2$  ratio for the mixed sample indicates the presence of shorter  $-\text{CH}_2-$  chains in it, presumably in the form of substituents on the aromatic skeleton.

The formation of oxygenated products is characterized by the complex broad band within the  $1800\text{--}1550\text{ cm}^{-1}$  spectral region (Figs 8a, 8b), exhibiting a somewhat different distribution of the carbonyl-containing species in the two samples, in particular a higher proportion of esters (band at about  $1770\text{ cm}^{-1}$ ) in the mixed sample, probably forming phenyl esters oxygen bridges in the oxidized organic matter.

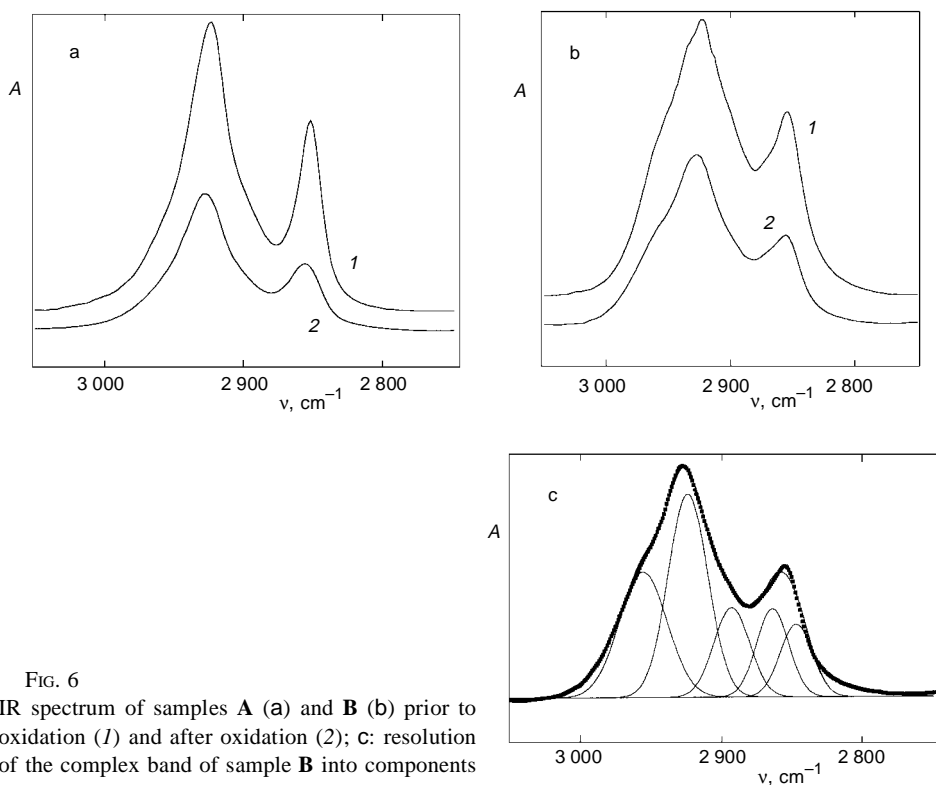


FIG. 6  
IR spectrum of samples **A** (a) and **B** (b) prior to oxidation (1) and after oxidation (2); c: resolution of the complex band of sample **B** into components



TABLE II  
Assignment of IR absorption bands within the C–H stretching region

Group	Band position		Assignment <sup>15</sup>
	present work	Painter <i>et al</i> <sup>5</sup>	
CH <sub>3</sub>	2 956	2 956	antisymmetric stretching <sup>a</sup>
	2 865	2 864	symmetric stretching
CH <sub>2</sub>	2 926	2 923	antisymmetric stretching <sup>b</sup>
	2 853	2 849	symmetric stretching
CH	2 893	2 891	stretching of lone CH bond

<sup>a</sup> Includes antisymmetric stretching vibrations of CH<sub>2</sub> groups in some hydroaromatic structures; <sup>b</sup> includes antisymmetric stretching vibrations of methyl groups attached to aromatic rings.

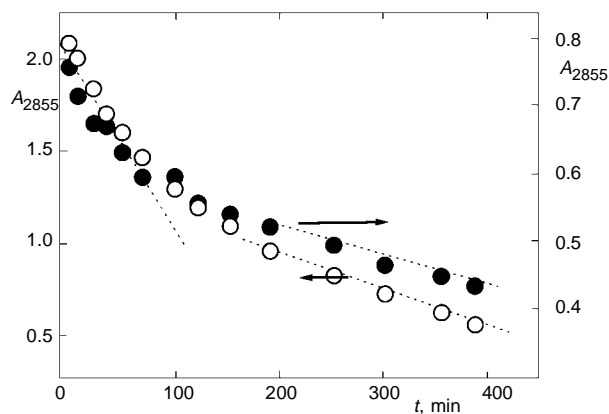


FIG. 7  
Time dependence of absorbance  $A$  at  $2\,855\text{ cm}^{-1}$  during oxidation. Sample:  $\circ$  A,  $\bullet$  B

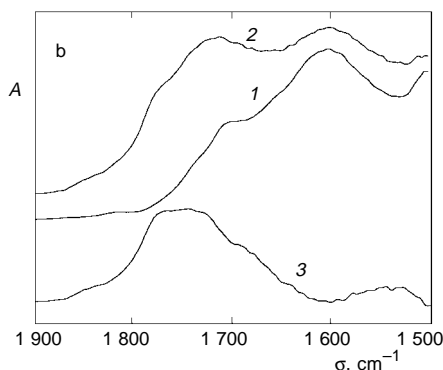
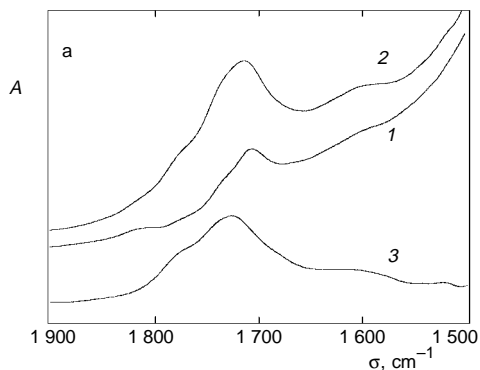


FIG. 8

IR spectra of samples A (a) and B (b) before (1) and after (2) oxidation; curve 3 is the difference between curves 1 and 2

The decrease in the pyrolysate yields can be explained in terms of formation of oxygen species on the surface of the organic matter particles. The oxygenated species (regenerated humic acids), rich in oxygen bridges, are very resistant to further pyrolysis<sup>16</sup>. Only small amounts of CO<sub>2</sub> and H<sub>2</sub>O are usually produced during pyrolysis<sup>17</sup>.

## CONCLUSIONS

Laboratory oxidation of fossil organic matter induces significant changes in its composition and properties, as indicated by the following effects:

1. The intensity of the bands due to the  $\nu(\text{CH}_3)$  and  $\nu(\text{CH}_2)$  stretching vibrations decreases during the oxidation, while that of bands characteristic for oxygenated species (ketones, aldehydes and, in particular, esters) increases substantially.

2. The Rock-Eval  $S_2/S_1$  ratio and the time dependence of intensities of the CH<sub>2</sub> and CH<sub>3</sub> stretching vibrations indicate that "free" hydrocarbons are preferentially evaporized and oxidized during first 8–16 h of the laboratory oxidation. After that period of time, hydrocarbons "bound" to the kerogen macromolecule are attacked.

3. In contrast to the natural maturation of organic matter, the Rock-Eval  $T_{\text{max}}$  values decrease during the laboratory oxidation, presumably due to the oxidative splitting of the kerogen structure.

4. The amount of the "off-line" liquid pyrolysis products decreases substantially during oxidation. The pyrolysis products of aliphatic and mixed organic matter consist mainly of long-chain aliphatic hydrocarbons, which indicates that the aliphatic part of the fossil organic matter is preferentially affected by the oxidation.

*This study was supported by the Grant Agency of the Czech Republic (Grant No. 205/95/0151).*

## REFERENCES

1. Jensen E. J., Melnyk N., Wood J., Berkowitz N.: *Adv. Chem. Ser.* 55, 621 (1964).
2. Dereppe J. M., Moreaux C., Landais P., Monthieux M.: *Fuel* 67, 764 (1987).
3. Seki H., Ito O., Limo M.: *Fuel* 69, 1047 (1990).
4. Painter P. C., Snyder R. W., Pearson D. E., Kwong J.: *Fuel* 59, 282 (1980).
5. Painter P. C., Coleman M. M., Snyder R. W., Mahajan O., Komatsu M., Walker P. L., Jr.: *Appl. Spectrosc.* 35, 106 (1981).
6. Buckmaster H. A., Kudynska J.: *Fuel* 71, 1137 (1992).
7. Clemens A. H., Matheson T. W., Rogers D. E.: *Fuel* 70, 215 (1991).
8. Huffman G. P., Huggins F. E., Dunmyre G. R., Pignocco A. J., Lin M.-C.: *Fuel* 64, 849 (1985).
9. Kalema W. S., Gavalas G. R.: *Fuel* 66, 158 (1987).
10. Durant B. in: *Kerogen–Organic Matter from Sedimentary Rocks*, p. 180. Editions Technique, Paris 1980.
11. Landais P., Monthieux M., Meunier J.-D.: *Org. Geochem.* 7, 249 (1984).
12. Cejka J., Holy L., Kribek B., Sedlacek V.: *Collect. Czech. Chem. Commun.* 61, 1158 (1996).

13. Cejka J., Sobalik Z., Holy L., Kribek B., Sedlacek V. in: *Weathering of Fossil Organic Matter* (B. Kribek, Ed.), p. 49. Czech Geological Survey, Prague 1996.
15. Anderson K. B., Johns R. B.: *Org. Geochem.* 9, 219 (1986).
16. Whitehurst D. D., Mitchell T. O., Farcasiu M. in: *Coal Liquefaction: The Chemistry and Technology of Thermal Process*, p. 112. Academic Press, New York 1980.
17. Ouchi K., Meada Y., Otoh H., Makabe M.: *Fuel* 63, 35 (1984).